A Doublet-Lattice Method Correction Approach for High Fidelity Gust Loads Analysis

C. Valente [*], Y. Lemmens[†]

Siemens Industry Software NV, B-3001 Leuven, Belgium

C. Wales [‡], D. Jones [§], A. L. Gaitonde [¶], J. E. Cooper[‖]

Department of Aerospace Engineering, University of Bristol, Bristol, BS8 1TR, U.K.

This paper presents a new methodology to increase the accuracy of gust loads analysis, evaluated by means of traditional potential flow models. Linearised frequency domain aerodynamic loads have been used to estimate the correction factors necessary to update the Aerodynamic Interference Coefficients matrices for gust and mode shapes deformation. The results, obtained using a corrected doublet-lattice method, are presented and compared to the fully coupled CFD/FEM results computed with a Fluid Structure Interaction interface. The application of this technique to a wing model, representative of a general single aisle civil aircraft, has shown an excellent agreement to the fully coupled results, both for rigid and flexible aerodynamic loads in the transonic regime.

Nomenclature

α	Angle of attack
ρ	Atmospheric density
H	distance parallel to the flight path of the airplane for the gust to reach its peak velocity
F_g	Flight profile alleviation factor
k	Reduced frequency
L_g	Gust wavelength
M	Mach number
$\bar{q}$	Flight dynamic pressure
U_{ds}	Design gust velocity in equivalent air speed (EAS)
U_{ref}	Reference gust velocity in EAS
W_g	Maximum gust velocity
x	Gust penetration
$\mathbf{A}_{jj}$	Aerodynamic influence coefficient matrix, $AICs$
$\mathbf{F}_a^{CFD}$	Aerodynamic integrate loads computed by CFD
$\mathbf{F}_a^{DLM}$	Aerodynamic integrate loads computed by DLM
$\widehat{\mathbf{F}}_a^{DLM}$	Aerodynamic integrate loads computed by corrected DLM
$\mathbf{F}_j^e$	α_0 contribution
$\mathbf{G}_{kr}^T$	Integration Matrix over the Aerodynamic Monitor Points
$\mathbf{PP}(\omega)$	Fourier Transform of the time domain gust disturbance defined by the user
$\mathbf{QARJ}^T$	Generalized aerodynamic influence coefficient matrix relating the downwash to the aerodynamic load on the monitor point

[*]Marie Curie Early Stage Research Fellow in Aircraft Loads. Email: carmine.valente@bristol.ac.uk

[†]Sr. Project Leader RTD, Digital Factory Division, Product Lifecycle Management, Simulation & Test Solutions. Email: yves.lemmens@siemens.com

[‡]Research Associate in Aeroelasticity/ Dynamics. Email: chris.wales@bristol.ac.uk

[§]Senior Lecturer in Aerodynamics. Email: dorian.jones@bristol.ac.uk

[¶]Senior Lecturer in Aerodynamics. Email: ann.gaitonde@bristol.ac.uk

[‖]RAEng Airbus Sir George White Professor of Aerospace Engineering. Email: j.e.cooper@bristol.ac.uk

$\mathbf{S}_{kj}$ Aerodynamic integration matrix
$\mathbf{W}_{jj}^{w}$ Correction factor matrix
$\mathbf{W}^{\epsilon}$ Weight matrix
$\mathbf{w}_{j}$ Downwash vector applied a the collocation points
$\mathbf{w}_{ja}^{MS}$ Downwash due to the mode shape deformation

Superscripts
S Steady aerodynamic loads
G Gust aerodynamic loads
MS Mode shape deformation aerodynamic loads

Subscripts
j Aerodynamic control point set (3/4 point of panel), equal to the number of aero panels
k Aerodynamic load point set (mid point on panel), twice the number of aero panels
a Structural grid point set
i Normal modes set
e Extra point set
h Combination of normal mode and extra point set

I. Introduction

The current industrial standard for gust loads modelling is to use traditional potential flow models, such as the doublet-lattice method (DLM) and strip theory,[1,2] to generate the air loads interacting with the aircraft structure. However the growing interest in flexible-aircraft dynamics has highlighted how these models make simplifying assumptions that may not allow an accurate prediction of the air loads in these cases. Since linear unsteady aerodynamics show inaccuracies in the transonic regime, where the linear assumptions are no longer valid and the effects of viscosity and thickness are relevant, many correction techniques have been developed in the past years[3,4] to attempt to address this issue. Their aim is to introduce wind tunnel data and Computational Fluid Dynamics (CFD) results into the linear unsteady aerodynamics[5,6] to give improved predictions in this flight regime. Unfortunately most of them rely on a large quantity of additional data. The increased availability of high performance computing, has seen the development of reliable fluid and structural solvers for use in the engineering design process.[7–9] In the aeroelastic domain, fluid structure interaction procedures are often considered as a means of replacing expensive experimental campaigns.

The work presented in this paper aims to present a new approach to correct the air loads computed using DLM for gust loads analysis. For many years the Doublet Lattice Method has been used as the reference method in the aerospace industry to compute unsteady aerodynamics. One of the main advantages that it offers is the low computational cost and the advantage that it can be integrated in the commercial aeroelastic solver Nastran. So, it has become the standard method to compute the aerodynamic loads interacting with the structure for gust analysis. However being based on the linearized potential equations, it doesn't describe effects related to thickness, shock wave formation or viscosity. Additionally, Tijdeman in[10] highlighted how the principle of superposition is not valid in the transonic regime, thus it is not possible to consider the steady and unsteady characteristics separately. In fact the unsteady aerodynamics depends explicitly upon the steady part.

Due to the fact that the DLM method cannot properly predict the aerodynamics in the transonic regime, where non linear effects become important, several techniques have been presented during the last decades to correct the aerodynamic coefficient influence matrix $AICs$. In particular, the industrial approach has been to match the steady results at zero frequency. The common idea, at the base of most of these correction methods, is to use nonlinear pressure distribution measured on the model, or computed with CFD analysis, to correct the result obtained from linear methods.

Combining the cheap computational cost of a lower order method, with the information obtained with an higher order method, it is possible to achieve a good compromise between performance and accuracy. This make possible the investigation of thousand of loads cases, necessary for flutter and dynamic flight loads, approximating the complex flow effects. Many attempts have been made to solve the transonic aeroelastic problem using combined procedures that relate linear models to measured data for the correction

of unsteady linear aerodynamics. These corrections can be performed by the multiplication, addition, or complete replacement of the aerodynamic influence coefficient matrix. The correction techniques, applied to unsteady loading calculation for static or dynamic stability analysis, can be classified in four major groups according to Silva.[11]

In 1976, Giesing, Kalman and Rodden,[5] published a report describing methods to correct lifting surface theory so that it could reflect known experimental data. The approach proposed was to define a matrix of correction factors, in order to better match experimental data while minimizing the change to the theoretical pressure distribution. One way to obtain this results is to use premultiplying or postmultiplying correction matrices applied to the AIC matrix. While the premultiplying can be considered as a correction on the pressure distribution, the postmultiplying could be regarded as a correction to the downwash to account for thickness effects and for camber induced by boundary-layer displacement effects. Silva[11] pointed out how a pressure based method, can presents problems due to the pressure ratio calculation in the presence of very low pressure coefficients. At that point the corrections can produce very high correction factors, resulting in a poor conditioning of the corrected matrix.

For the present work a post multiplying approach has been preferred to a pre multiplying method, even considering that a good representation of the shock position and movement is not achievable mainly due to the low refinements in the aerodynamic panel discretization. On the other hand, the present approach will attempt to close the gap between the aerodynamic integrated loads that the panel method transfers onto the structure and the loads computed from a higher fidelity analysis environment.

II. Doublet-Lattice Method Correction Approach

A. AICs Correction for steady aeroelasticity

The steady aeroelastic integrated loads computed from the baseline doublet-lattice method[12] can be expressed as:

$$\mathbf{F}_a^{DLM_S} = \bar{q}\mathbf{G}_{kr}^T\mathbf{S}_{kj}\mathbf{A}_{jj}^{-1}\mathbf{w}_j^{DLM} \tag{1}$$

where

$\bar{q}$	dynamic pressure
$\mathbf{G}_{kr}^T$	integration matrix over the aerodynamic monitor points
$\mathbf{S}_{kj}$	aerodynamic integration matrix
$\mathbf{A}_{jj}$	aerodynamic influence coefficient matrix, $AICs$
$\mathbf{w}_j^{DLM}$	downwash matrix

however, it is possible to define a corrected DLM introducing a post multiplying correction matrix and considering the contribution of the forces at zero angle of attack:

$$\widehat{\mathbf{F}}_a^{DLM_S} = \bar{q}\mathbf{G}_{kr}^T\mathbf{S}_{kj}\mathbf{A}_{jj}^{-1}\ \mathbf{W}_{jj}^w\mathbf{w}_j^{DLM} + \bar{q}\mathbf{G}_{kr}^T\mathbf{S}_{kj}\mathbf{F}_j^e \tag{2}$$

where

$\mathbf{W}_{jj}^w$	correction factor matrix
$\mathbf{F}_j^e$	α_0 contribution

The aim of this correction approach is to match the integrated steady aerodynamic loads acting on the structural nodes computed from the CFD code:

$$\mathbf{F}_a^{CFD_S} = \widehat{\mathbf{F}}_a^{DLM_S} \tag{3}$$

these can be expanded as follow:

$$\mathbf{F}_a^{CFD_S} = \bar{q}\mathbf{G}_{kr}^T\mathbf{S}_{kj}\mathbf{A}_{jj}^{-1}\ \mathbf{W}_{jj}^w\mathbf{w}_j^{DLM} + \bar{q}\mathbf{G}_{kr}^T\mathbf{S}_{kj}\mathbf{F}_j^e \tag{4}$$

The correction process aims to find the matrices $\mathbf{W}_{jj}^w$ and $\mathbf{F}_j^e$ such that the sectional loads computed with the DLM method match the CFD loads. There aren't a unique pair of matrices that can be used to

correct the DLM, so the idea is to find two matrices that minimise the change to the DLM solution. The aim is to find a $\mathbf{F}_j^e$ as close as possible to zero and a matrix $\mathbf{W}_{jj}^w$ as close to the identity matrix as possible.

This means minimising the weighted sum of the square of the deviations, where the deviation $\mathbf{W}_{jj}^w$ is defined as the difference between the correction factor and unity

$$\mathbf{W}_{jj}^w = \begin{bmatrix} \ddots & & \\ & \mathbf{I} + \boldsymbol{\epsilon}^w & \\ & & \ddots \end{bmatrix} \tag{5}$$

This leads to an under determined problem, with two unknowns to be minimised:

$$\mathbf{F}_a^{CFD_S} = \bar{q}\mathbf{G}_{kr}^T\mathbf{S}_{kj}\mathbf{A}_{jj}^{-1}\lceil\mathbf{I} + \boldsymbol{\epsilon}^w\rfloor\mathbf{w}_j^{DLM} + \bar{q}\mathbf{G}_{kr}^T\mathbf{S}_{kj}\mathbf{F}_j^e \tag{6}$$

The equations can be rewritten as follow:

$$\mathbf{F}_a^{CFD_S} = \bar{q}\mathbf{G}_{kr}^T\mathbf{S}_{kj}\mathbf{A}_{jj}^{-1}\mathbf{I}\mathbf{w}_j^{DLM} + \bar{q}\mathbf{G}_{kr}^T\mathbf{S}_{kj}\mathbf{A}_{jj}^{-1}\boldsymbol{\epsilon}^w\mathbf{w}^{DLM} + \bar{q}\mathbf{G}_{kr}^T\mathbf{S}_{kj}\mathbf{F}_j^e \tag{7}$$

where the first therm at the right hand side is the uncorrected DLM.

$$\mathbf{F}_a^{CFD_S} = \mathbf{F}_a^{DLM_S} + \bar{q}\mathbf{G}_{kr}^T\mathbf{S}_{kj}\mathbf{A}_{jj}^{-1}\boldsymbol{\epsilon}^w\mathbf{w}^{DLM} + \bar{q}\mathbf{G}_{kr}^T\mathbf{S}_{kj}\mathbf{F}_j^e \tag{8}$$

So defining a delta between the CFD and DLM strip loads:

$$\Delta\mathbf{F}_a^S = \mathbf{F}_a^{CFD_S} - \mathbf{F}_a^{DLM_S} \tag{9}$$

$$\Delta\mathbf{F}_a^S = \bar{q}\mathbf{G}_{kr}^T\mathbf{S}_{kj}\mathbf{A}_{jj}^{-1}\boldsymbol{\epsilon}^w\mathbf{w}_j^{DLM} + \bar{q}\mathbf{G}_{kr}^T\mathbf{S}_{kj}\mathbf{F}_j^e \tag{10}$$

This under determined problem can be solved using a least squares approach. However, it is necessary to calculate the DLM downwash, which for a static trim analysis comprises two contributions:

$$\mathbf{w}_j^{DLM} = \mathbf{D}_{jk}\mathbf{G}_{ka}\mathbf{u}_a + \mathbf{D}_{jx}\mathbf{u}_x \tag{11}$$

The first term at the right hand side of Eq. (11) is due to the presence of the structural deformation, while the second is related to the presence of the unity displacement of the aeroelastic extra point. Replacing Eq. (11) in Eq. (2) it is possible to write the corrected DLM contribution as:

$$\widehat{\mathbf{F}}_a^{DLM_S} = \bar{q}\mathbf{G}_{kr}^T\mathbf{S}_{kj}\mathbf{A}_{jj}^{-1}\ \mathbf{W}_{jj}^w\mathbf{D}_{jk}\mathbf{G}_{ka}\mathbf{u}_a + \bar{q}\mathbf{G}_{kr}^T\mathbf{S}_{kj}\mathbf{A}_{jj}^{-1}\ \mathbf{W}_{jj}^w\mathbf{D}_{jx}\mathbf{u}_x + \bar{q}\mathbf{G}_{kr}^T\mathbf{S}_{kj}\mathbf{F}_j^e \tag{12}$$

From Eq. (12) it is possible to extract the expression of the aerodynamic forces for a rigid aeroelastic system:

$$\widehat{\mathbf{F}}_{a_R}^{DLM_S} = \bar{q}\mathbf{G}_{kr}^T\mathbf{S}_{kj}\mathbf{A}_{jj}^{-1}\mathbf{W}_{jj}^w\mathbf{D}_{jx}\mathbf{u}_x + \bar{q}\mathbf{G}_{kr}^T\mathbf{S}_{kj}\mathbf{F}_j^e \tag{13}$$

and the contribution of the elastic increment:

$$\widehat{\mathbf{F}}_{a_E}^{DLM_S} = \bar{q}\mathbf{G}_{kr}^T\mathbf{S}_{kj}\mathbf{A}_{jj}^{-1}\mathbf{W}_{jj}^w\mathbf{D}_{jk}\mathbf{G}_{ka}\mathbf{u}_a \tag{14}$$

In order to compute the correction coefficients, $\boldsymbol{\epsilon}^w$, and the zero angle of attack contribution, $\mathbf{F}_j^e$, it is necessary to solve Eq. (10) for two reference conditions. In the present work the flight shape of the wing is not known, for this reason a first correction step will consider just the rigid aerodynamic forces.

Considering a wing clamped at the root, without any control surfaces, the only aeroelastic extra point is the angle of attack:

$$\mathbf{u}_x = \{\alpha\} \tag{15}$$

At this point Eq. (10) can be solved for two flight conditions at different angle of attack: the first considering an angles of attack of $0°$, and the second at the flight incidence of the reference condition at which the loads are required, $\alpha = 2°$.

$$\Delta\mathbf{F}_a^{S_1} = \bar{q}\mathbf{G}_{kr}^T\mathbf{S}_{kj}\mathbf{A}_{jj}^{-1}\boldsymbol{\epsilon}^w\mathbf{D}_{jx}\mathbf{u}_x^1 + \bar{q}\mathbf{G}_{kr}^T\mathbf{S}_{kj}\mathbf{F}_j^e \tag{16}$$

$$\Delta\mathbf{F}_a^{S_2} = \bar{q}\mathbf{G}_{kr}^T\mathbf{S}_{kj}\mathbf{A}_{jj}^{-1}\boldsymbol{\epsilon}^w\mathbf{D}_{jx}\mathbf{u}_x^2 + \bar{q}\mathbf{G}_{kr}^T\mathbf{S}_{kj}\mathbf{F}_j^e \tag{17}$$

this system can be written in a matrix format and solved in a least square sense:

$$\begin{Bmatrix} \Delta\mathbf{F}_a^{S_1} \\ \Delta\mathbf{F}_a^{S_2} \end{Bmatrix} = \begin{bmatrix} \bar{q}\mathbf{G}_{kr}^T\mathbf{S}_{kj}\mathbf{A}_{jj}^{-1}\mathbf{D}_{jx}\mathbf{u}_x^1 & \bar{q}\mathbf{G}_{kr}^T\mathbf{S}_{kj} \\ \bar{q}\mathbf{G}_{kr}^T\mathbf{S}_{kj}\mathbf{A}_{jj}^{-1}\mathbf{D}_{jx}\mathbf{u}_x^2 & \bar{q}\mathbf{G}_{kr}^T\mathbf{S}_{kj} \end{bmatrix} \begin{Bmatrix} \boldsymbol{\epsilon}^w \\ \mathbf{F}_j^e \end{Bmatrix} \tag{18}$$

The solution of the minimization problem allows the computation of the rigid and elastic aerodynamic integrated loads computed by the corrected DLM using Eq. (13) and Eq. (14).

B. AICs Correction fur Gust Response Analysis

The aeroelastic frequency response analysis in modal coordinates, as implemented in the Nastran solver, is based on the solution of the following equation:

$$\left[-\omega^2\mathbf{M}_{hh} + i\omega\mathbf{B}_{hh} + (1+ig)\ \mathbf{K}_{hh} - \bar{q}\mathbf{Q}_{hh}(M,k)\right]\mathbf{U}_h = \bar{q}w_g\mathbf{PP}(\omega)\mathbf{Q}_{hj}(M,k)\mathbf{w}_j(\omega) \tag{19}$$

where two are the terms that account for the aerodynamic loads due to a gust disturbance:

$$\mathbf{Q}_{hh}(M,k) = \boldsymbol{\phi}_{ah}^T\mathbf{G}_{ka}^T\mathbf{S}_{kj}\ \mathbf{A}_{jj}^{-1}\ \mathbf{D}_{jk}\mathbf{G}_{ka}\boldsymbol{\phi}_{ah} \tag{20}$$

and due to a structural deformation:

$$\mathbf{Q}_{hj}(M,k) = \boldsymbol{\phi}_{ah}^T\mathbf{G}_{ka}^T\mathbf{S}_{kj}\ \mathbf{A}_{jj}^{-1} \tag{21}$$

These two contribution are linearly added to evaluate the total aerodynamic loads. For this reason, the presented correction method correct first the rigid gust loads and then the aerodynamic load obtained from a mode shape deformation.

1. AICs Correction using Sinusoidal Gusts

The aim of this correction approach is to match the integrated aerodynamic loads acting on the structural nodes computed from the CFD code for a sinusoidal gust shape. Following a similar process as seen in the previous section:

$$\mathbf{F}_a^{CFD_G} = \widehat{\mathbf{F}}_a^{DLM_G} \tag{22}$$

where the right hand side term can be expanded for the corrected Doublet Lattice Method,[12] as follow:

$$\mathbf{F}_a^{CFD_G} = \bar{q}w_g\mathbf{PP}(\omega)\mathbf{G}_{kr}^T\mathbf{S}_{kj}\ \mathbf{A}_{jj}^{-1}\mathbf{W}_{jj}^w\mathbf{w}_j(\omega) \tag{23}$$

and

$\bar{q}$	dynamic pressure
w_g	gust scaling factor
$\mathbf{PP}(\omega)$	Fourier Transform of the time domain gust disturbance defined by the user
$\mathbf{G}_{kr}^T$	integration matrix over the aerodynamic monitor points
$\mathbf{S}_{kj}$	aerodynamic integration matrix
$\mathbf{A}_{jj}$	aerodynamic influence coefficient matrix, $AICs$
$\mathbf{W}_{jj}^w$	correction coefficients matrix
$\mathbf{w}_j$	downwash matrix

The downwash contribution is a matrix defined as follow

$$\mathbf{w}_j(\omega_i) = \cos\gamma_j e^{-i\omega_i(x_j-x_0)/U_\infty} \qquad \text{with } i = 1,\cdots,N_f \tag{24}$$

where:

ω_i	excitation frequency, or gust frequency
γ_j	dihedral angle of the j-th aerodynamic element
x_j	x-location of the j-th aerodynamic element in the aerodynamic coordinate system
x_0	reference coordinate for the gust

Defining the generalized aerodynamic influence coefficient matrix relating the downwash to the aerodynamic loads on the monitor points, which correspond to the CFD strips being matched:

$$\mathbf{QARJ}^T = \mathbf{G}_{kr}^T \mathbf{S}_{kj}\ \mathbf{A}_{jj}^{-1} \tag{25}$$

it is possible to rewrite

$$\mathbf{F}_a^{CFD_G} = \bar{q} w_g \mathbf{PP}(\omega) \mathbf{QARJ}^T \mathbf{W}_{jj}^w \mathbf{w}_j(\omega) \tag{26}$$

Considering a time gust disturbance with a sinusoidal shape, the Fourier Transform comes to be a vector with only one non zero component, corresponding to the frequency of the input signal. Expanding Eq. 26 for a single frequency, it is a possible to write:

$$\mathbf{F}_a^{CFD_G} = \bar{q} w_g \mathbf{QARJ}^T \mathbf{W}_{jj}^w \bar{\mathbf{w}}_j^G \tag{27}$$

Considering a diagonal correction matrix, as in Eq. (5), Eq. (27) can be written as:

$$\mathbf{F}_a^{CFD_G} = \mathbf{F}_a^{DLM_G} + \bar{q} w_g \mathbf{QARJ}^T \begin{bmatrix} \ddots & & \\ & \boldsymbol{\epsilon}^w & \\ & & \ddots \end{bmatrix} \bar{\mathbf{w}}_j^G \tag{28}$$

so that it is possible to express the change in aerodynamic loads as:

$$\Delta\mathbf{F}_a^G = \bar{q} w_g \mathbf{QARJ}^T \begin{bmatrix} \ddots & & \\ & \bar{\mathbf{w}}_j^G & \\ & & \ddots \end{bmatrix} \{\boldsymbol{\epsilon}^w\} \tag{29}$$

and introducing the following matrix:

$$\mathbf{QP} = w_g \mathbf{QARJ}^T \begin{bmatrix} \ddots & & \\ & \bar{\mathbf{w}}_j^G & \\ & & \ddots \end{bmatrix} \tag{30}$$

$$\Delta\mathbf{F}_a^G = \bar{q} \mathbf{QP} \{\boldsymbol{\epsilon}^w\} \tag{31}$$

All the matrices and vectors in Eq. (31) are complex, so it possible to rewrite it as:

$$\Re(\Delta\mathbf{F}_a^G) + i\Im(\Delta\mathbf{F}_a^G) = \bar{q}[\Re(\mathbf{QP}) + i\Im(\mathbf{QP})]\{\Re(\boldsymbol{\epsilon}^w) + i\Im(\boldsymbol{\epsilon}^w)\} \tag{32}$$

Using the following notation:

$$\begin{aligned} \Re(\Delta\mathbf{F}_a^G) &= \Delta\mathbf{F}_a{}^{R^G} \\ \Im(\Delta\mathbf{F}_a^G) &= \Delta\mathbf{F}_a{}^{I^G} \\ \Re(\mathbf{QP}) &= \mathbf{QP}^R \\ \Im(\mathbf{QP}) &= \mathbf{QP}^I \\ \Re(\boldsymbol{\epsilon}^w) &= \boldsymbol{\epsilon}^R \\ \Im(\boldsymbol{\epsilon}^w) &= \boldsymbol{\epsilon}^I \end{aligned} \tag{33}$$

$$\begin{aligned} \Delta\mathbf{F}_a^{R^G} + i\Delta\mathbf{F}_a^{I^G} &= \bar{q}\Big(\mathbf{QP}^R + i\mathbf{QP}^I\Big)\Big(\boldsymbol{\epsilon}^R + i\boldsymbol{\epsilon}^I\Big) \\ &= \bar{q}\Big(\mathbf{QP}^R\boldsymbol{\epsilon}^R + i\mathbf{QP}^R\boldsymbol{\epsilon}^I + i\mathbf{QP}^I\boldsymbol{\epsilon}^R - \mathbf{QP}^I\boldsymbol{\epsilon}^I\Big) \end{aligned} \tag{34}$$

It is possible to write this equation in a matrix format obtaining

$$\begin{Bmatrix} \Delta\mathbf{F}_a^{R^G} \\ \Delta\mathbf{F}_a^{I^G} \end{Bmatrix} = \bar{q} \begin{bmatrix} \mathbf{QP}^R & -\mathbf{QP}^I \\ \mathbf{QP}^I & \mathbf{QP}^R \end{bmatrix} \begin{Bmatrix} \boldsymbol{\epsilon}^R \\ \boldsymbol{\epsilon}^I \end{Bmatrix} \tag{35}$$

Solving in a least square sense it is possible to determine the correction factors and obtain the correction matrix for each reduced frequency.

2. Weighting Correction Method

It is possible to use a weighting in the least square solution of Eq. (35). As a first approach, it has been decided to use the uncorrected $AICs$ matrix as the weight. Introducing a new variable:

$$\boldsymbol{\epsilon} = \mathbf{W}^{\epsilon}\, \widehat{\boldsymbol{\epsilon}} \tag{36}$$

where the matrix $\mathbf{W}^{\epsilon}$ is defined as

$$\mathbf{W}^{\epsilon} = \begin{bmatrix} \mathbf{W}^{\epsilon R} & 0 \\ 0 & \mathbf{W}^{\epsilon I} \end{bmatrix} \tag{37}$$

where $\mathbf{W}^{\epsilon^R}$ and $\mathbf{W}^{\epsilon^I}$ are the real and imaginary weightings given by

$$\mathbf{W}^{\epsilon R} = \begin{bmatrix} \ddots & & \\ & |\mathbf{A}_{jj}^{-1^R}\, \mathbf{I}| & \\ & & \ddots \end{bmatrix} \qquad \mathbf{W}^{\epsilon I} = \begin{bmatrix} \ddots & & \\ & |\mathbf{A}_{jj}^{-1^I}\, \mathbf{I}| & \\ & & \ddots \end{bmatrix} \tag{38}$$

where the $\mathbf{I}$ is a vector of ones. Substituting Eq. (36) and Eq. (37) in Eq. (35), the new system to solve at this point become

$$\begin{Bmatrix} \Delta\mathbf{F}_a^{R^G} \\ \Delta\mathbf{F}_a^{I^G} \end{Bmatrix} = \bar{q} \begin{bmatrix} \mathbf{QP}^R & -\mathbf{QP}^I \\ \mathbf{QP}^I & \mathbf{QP}^R \end{bmatrix} \begin{bmatrix} \mathbf{W}^{\epsilon R} & 0 \\ 0 & \mathbf{W}^{\epsilon I} \end{bmatrix} \begin{Bmatrix} \widehat{\boldsymbol{\epsilon}}^R \\ \widehat{\boldsymbol{\epsilon}}^I \end{Bmatrix} \tag{39}$$

C. AICs Correction using Harmonic Mode Shape

The aerodynamic strip loads due to an harmonic mode deformation of the structure, in the frequency domain, calculated using the DLM can be expressed as

$$\mathbf{F}_a^{DLM_{MS}} = \bar{q}\mathbf{G}_{kr}^T\mathbf{S}_{kj}\ \mathbf{A}_{jj}^{-1}\mathbf{w}_{ja}^{MS} \tag{40}$$

where the downwash due to the mode shape deformation is given by:

$$\mathbf{w}_{ja}^{MS} = (\mathbf{D}_{jk}^1 + ik\mathbf{D}_{jk}^2)\mathbf{G}_{ka}^T\tilde{\mathbf{u}}_a \tag{41}$$

where $\tilde{\mathbf{u}}_a$ is the Fourier transform of the structural mode deformation time history, given by the product of the mode amplitude and a vector defining the time history of the harmonic shape variation:

$$\tilde{\mathbf{u}}_a = \mathcal{F}(\mathbf{u}_a(t)) \tag{42}$$

Using the same approach as the gust correction we can introduce a correction matrix to match the mode shape loads calculated with CFD, leading to the equation:

$$\mathbf{F}_a^{CFD_{MS}} = \bar{q}\mathbf{G}_{kr}^T\mathbf{S}_{kj}\ \mathbf{A}_{jj}^{-1}\mathbf{W}_{jj}^w\mathbf{w}_{ja}^{MS} \tag{43}$$

Using Eq. (25) it is possible to rewrite Eq. (43) as:

$$\mathbf{F}_a^{CFD_{MS}} = \bar{q}\mathbf{QARJ}^T\mathbf{W}_{jj}^w\mathbf{w}_{ja}^{MS} \tag{44}$$

and using the same diagonal definition for $\mathbf{W}_{jj}^w$ as Eq. (5), the delta aerodynamic loads can be expressed as:

$$\Delta\mathbf{F}_a^{MS} = \bar{q}\mathbf{QARJ}^T \begin{bmatrix} \ddots & & \\ & \boldsymbol{\epsilon}^w & \\ & & \ddots \end{bmatrix} \{\mathbf{w}_{ja}^{MS}\} = \bar{q}\mathbf{QARJ}^T \begin{bmatrix} \ddots & & \\ & \mathbf{w}_{ja}^{MS} & \\ & & \ddots \end{bmatrix} \{\boldsymbol{\epsilon}^w\} \tag{45}$$

$$\mathbf{QW} = \mathbf{QARJ}^T \begin{bmatrix} \ddots & & \\ & \mathbf{w}_{ja}^{MS} & \\ & & \ddots \end{bmatrix} \tag{46}$$

$$\Delta\mathbf{F}_a^{MS} = \bar{q}\mathbf{QW}\{\boldsymbol{\epsilon}^w\} \tag{47}$$

proceeding in an analogus way to what is done in Eq.(32), introducing the notation:

$$\begin{aligned} \Re(\mathbf{QW}) &= \mathbf{QW}^R \\ \Im(\mathbf{QW}) &= \mathbf{QW}^I \end{aligned} \tag{48}$$

$$\Delta\mathbf{F}_a^{R^{MS}} + i\Delta\mathbf{F}_a^{I^{MS}} = \bar{q}\Big(\mathbf{QW}^R\boldsymbol{\epsilon}^R + i\mathbf{QW}^R\boldsymbol{\epsilon}^I + i\mathbf{QW}^I\boldsymbol{\epsilon}^R - \mathbf{QW}^I\boldsymbol{\epsilon}^I\Big) \tag{49}$$

$$\begin{Bmatrix} \Delta\mathbf{F}_a^{R^{MS}} \\ \Delta\mathbf{F}_a^{I^{MS}} \end{Bmatrix} = \bar{q} \begin{bmatrix} \mathbf{QW}^R & -\mathbf{QW}^I \\ \mathbf{QW}^I & \mathbf{QW}^R \end{bmatrix} \begin{Bmatrix} \boldsymbol{\epsilon}^R \\ \boldsymbol{\epsilon}^I \end{Bmatrix} \tag{50}$$

In this case only one mode has been considered, but the system can be extended to additional mode shape deformation. In particular, tests have demonstrated that the best results are obtained when the flexible contribution correction factors, are computed considering both the gust and the mode shape deformation:

$$\begin{Bmatrix} \Delta\mathbf{F}_a^{R^G} \\ \Delta\mathbf{F}_a^{R^G} \\ \Delta\mathbf{F}_a^{R^{MS^n}} \\ \Delta\mathbf{F}_a^{I^{MS^n}} \end{Bmatrix} = \bar{q} \begin{bmatrix} \mathbf{QP}^R & -\mathbf{QP}^I \\ \mathbf{QP}^I & \mathbf{QP}^R \\ \mathbf{QW}^{R^n} & -\mathbf{QW}^{I^n} \\ \mathbf{QW}^{I^n} & \mathbf{QW}^{R^n} \end{bmatrix} \begin{Bmatrix} \boldsymbol{\epsilon}^R \\ \boldsymbol{\epsilon}^I \end{Bmatrix} \quad with \quad n = 1, ..., N^{modes} \tag{51}$$

In this case no weighting approach has been considered.

III. Correction method application

In order to fit the strip loads approach discussed in the previous sections, both the panel and the CFD mesh, have been divided into ten strips along the span. Each strip is defined around a structural grid node as shown in figure 2. The integrated loads computed from the CFD analysis, for each strip, become the target loads that the low fidelity method should be able to predict.

A. Aeroelastic model

A full aircraft beam stick FE model with lumped masses, representative of a single-aisle civil jet airliner, was developed as part of the FFAST project,[13] figure 1a . From this, the right wing model has been extracted and considered clamped at the root, figure 1b. The FFAST right wing model contains 10 beam elements for a total of 11 structural grid points, while the aerodynamic panel model counts of 11 boxes in the chord wise direction and 45 boxes in span, for a total of 495 aerodynamic panels. The panel method used in this investigation is the Doublet-Lattice Method available in the commercial solver Nastran. The wing CFD model (created using aerofoil data available for the three sections: root, crank and tip) does not include the engine and pylon, and has 33227 surface grid points, figure 1c. The CFD model has been solved using Euler equations. The flight condition used in the investigation is a $1g$ condition at an altitude of 11000 m, Mach number $M = 0.85$.

The range of frequency considered for the gust analysis is from 0 to 30 Hz. The FFAST right wing model considered has 13 mode of vibration in this range of frequency.

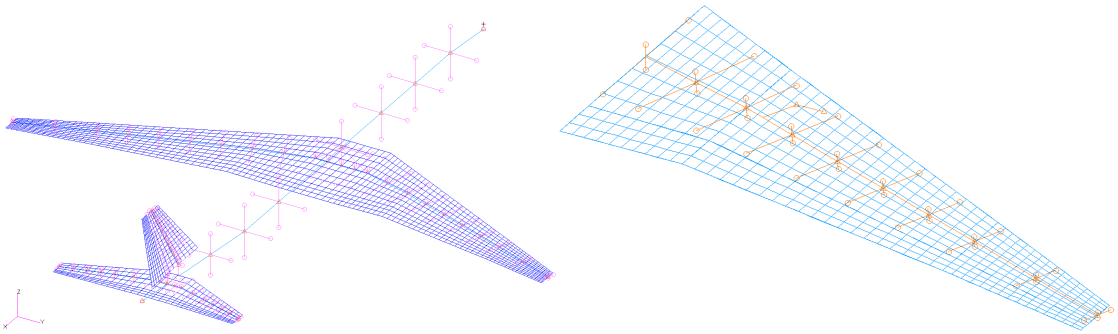

(a) Full FFAST FE beam stick type and DLM model.

(b) FFAST right wing FE and DLM model.

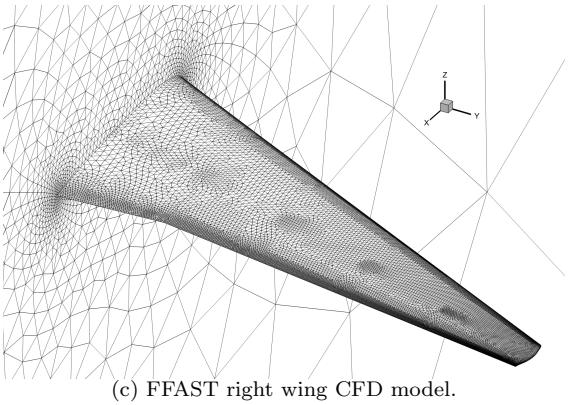

(c) FFAST right wing CFD model.

Figure 1: FFAST aeroelastic model.

B. Strongly coupled aeroelastic analysis using the AlpesFSI interface

The need for a high fidelity analysis environment, able to compute steady and unsteady aeroelastic computation, has driven the definition of a new Fluid Structure Interface, called AlpesFSI.[14] This interface provides a means to combine the finite element analysis with the loads computed from an external computational fluid dynamic solver(CFD). In the current case the CFD code chosen has been the DLR TAU-code.[15] From the trim configuration a transient analysis has been performed to compute the gust loads which the structure is subject to. The gust is modelled in TAU, using a field velocity method.[16–18] It is prescribed to start just outside the computational domain and travel at free stream velocity U_∞. The AlpesFSI interface has been used to study the aeroelastic trim deformation and the gust response of the FFAST right wing model clamped at the root, for the FEM, and a CFD model created in the jig shape of the structure.

C. Static aeroelastic correction

The aim of the steady correction approach is to match the aeroelastic loads at trim computed using AlpesFSI interface.[14] Assuming that the trim flight shape is not known in advance, the correction method has been used to match the aerodynamic loads computed in the undeformed jig shape (Flight Shape 1, FS1). The system at Eq. (18) is solved considering the CFD reference loads computed at two different angle of attack, $0°$ and $2°$. In figure 3 the vertical force and pitching moment, for the undeformed CFD model, are compared to the baseline and corrected DLM. In this case the corrected DLM, perfectly match the rigid CFD strip load. However this initial correction does not allow to obtain an accurate estimation of the elastic loads at the desired flight condition at $\alpha = 2°$, figure 4.

In order to increase the accuracy of the corrected method, a second correction step has been considered: using Eq. (10) and computing the strip loads using the CFD deformed at the flight shape computed at the previous step. As shown in figure 4, the corrected DLM for FS2 is very close to the loads computed using the AlpesFSI interface.

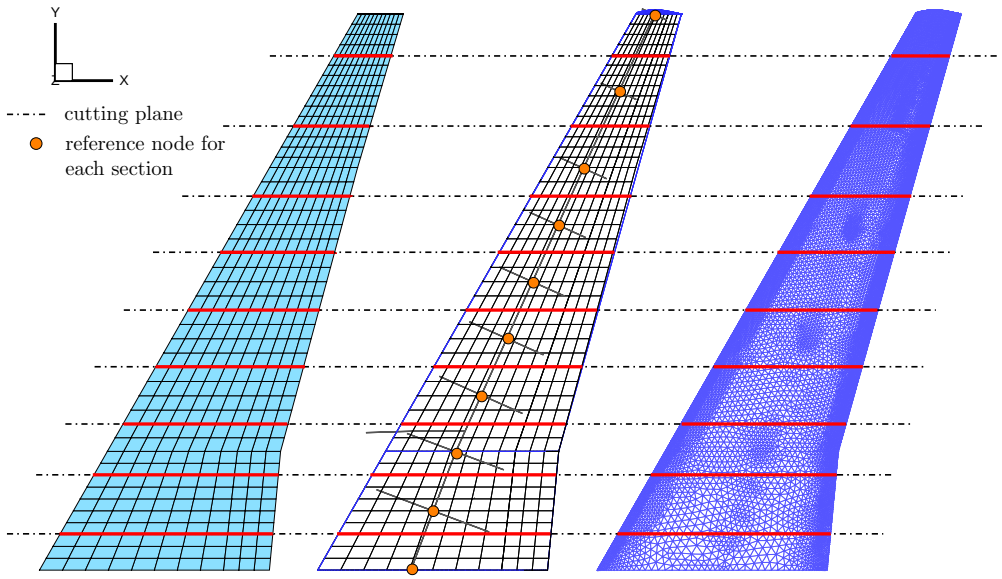

(a) DLM panel model (b) FEM model (c) CFD model

Figure 2: Comparison of DLM and CFD mesh, showing the sectional cutting planes and structural nodes along the wing aperture, used as reference points in the moment's calculation.

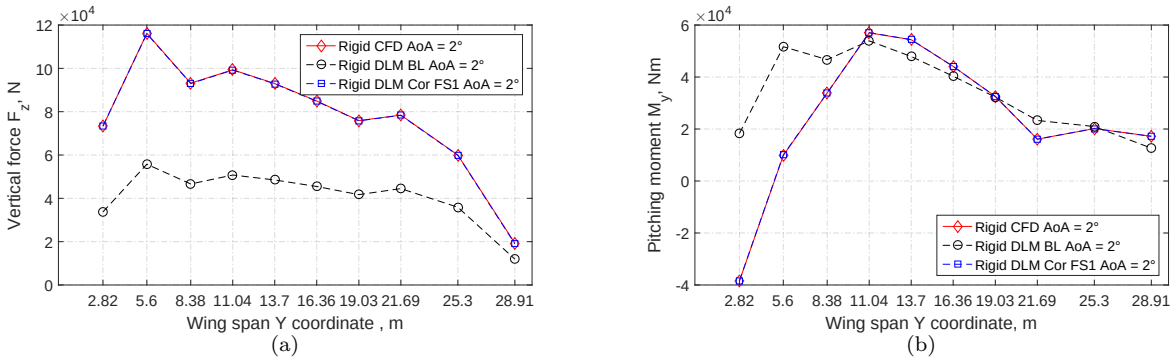

Figure 3: Rigid strip loads comparison for the undeformed flight shape at $\alpha = 2°$

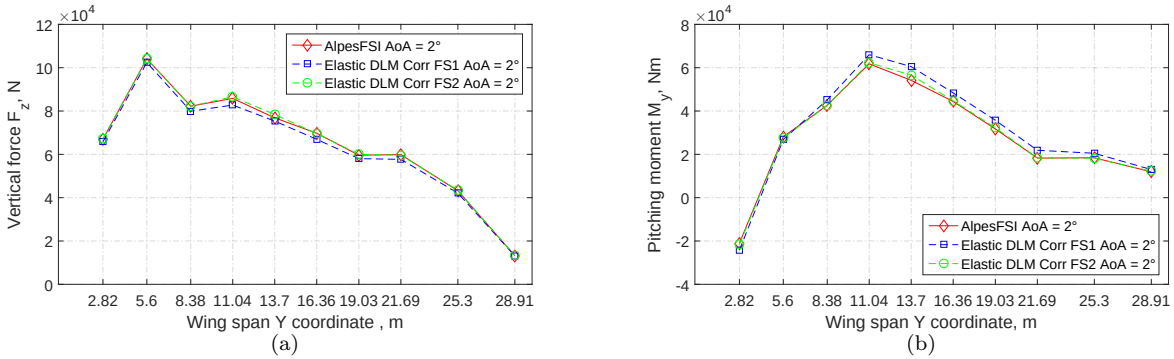

Figure 4: Trim strip loads comparison at $\alpha = 2°$.

D. CFD integrated loads in the frequency domain

The method described in the present work has been intended for Linear Frequency Domain Analysis (LFD)[19,20] . However, since LFD for gust were not available in the standard release of the CFD TAU code, when this method was being developed, equivalent frequency domain analysis has been recreated using time domain CFD analysis.

To compute the linearised frequency domain CFD loads, the rigid CFD response to a gust input has been studied in the CFD code DLR TAU. To remain in the linear region a small gust amplitude, equivalent to a $\alpha_g = 0.25°$, has been chosen. Different gust lengths have been chosen to match different reduced frequencies:

$$k = \frac{\omega_g}{U_\infty}\frac{l_{ref}}{2} = \frac{2\pi f_g}{U_\infty}\frac{l_{ref}}{2} \tag{52}$$

where the gust frequency f_g is dependent on the gust length:

$$f_g = \frac{U_{inf}}{L_g} \tag{53}$$

Table 1: List of reduced frequency used to perform the gust analysis in the frequency domain, with corresponding gust frequency and gust length.

k	$f_g\ [Hz]$	$L_g\ [m]$	k	$f_g\ [Hz]$	$L_g\ [m]$
0.01	0.13	1906.95	0.50	6.58	38.14
0.02	0.26	953.47	0.60	7.89	31.78
0.03	0.39	635.65	0.70	9.21	27.24
0.04	0.53	476.74	0.80	10.52	23.84
0.05	0.66	381.39	0.90	11.84	21.19
0.06	0.79	317.82	1.00	13.15	19.07
0.07	0.92	272.42	1.10	14.47	17.34
0.08	1.05	238.37	1.20	15.78	15.89
0.09	1.18	211.88	1.30	17.10	14.67
0.10	1.32	190.69	1.40	18.41	13.62
0.20	2.63	95.35	1.50	19.73	12.71
0.30	3.95	63.56	2.00	26.30	9.53
0.40	5.26	47.67			

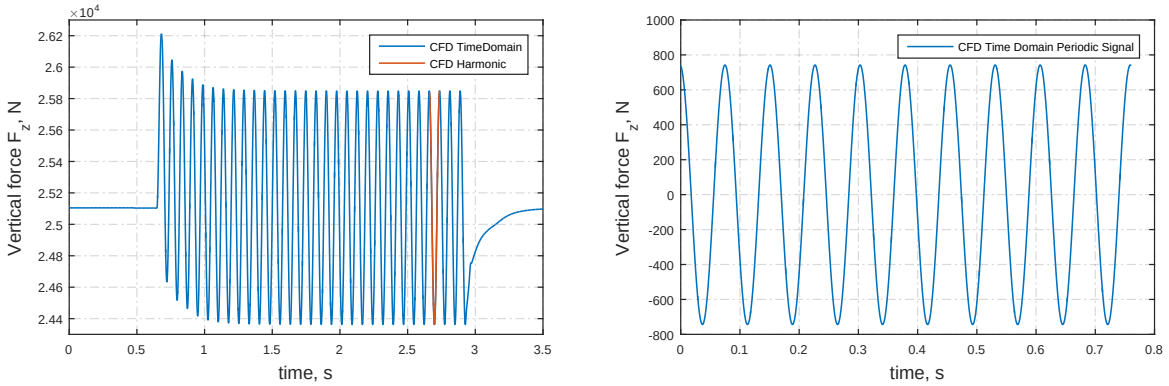

(a) CFD Time Domain Gust Response

(b) CFD Periodic Signal

Figure 5: Rigid CFD sinusoidal gust response.

The time domain CFD gust response loads has been evaluated for a series of reduced frequencies from $k = 0.01$ to $k = 2.0$, as reported in table 1. For each of them the time history of the integrated loads for the ten strips along the wing has been computed. The input signal has been chosen long enough to reach a stationary harmonic response. At this point a reference period has been selected, and an equivalent periodic signal has been reconstructed, figure 5. To obtain comparable results to the ones computed by the DLM the Fourier Series has been used to obtain the frequency domain loads.[12] The correction factors have been computed solving the system at Eq. (51) for each of the reduced frequency analysed.

E. "1-COS" Gust Response Analysis

The correction factors computed, as from the previous sections, have been used to update the $AICs$ matrices computed in the gust response analysis. The corrected $AICs$ matrices evaluated in the pre-processing step have been stored in a ".OP4" format and used to replace the $AICs$ matrices computed by Nastran at the running time. From this point the gust analysis can be performed to investigate the response to a typical one minus cosine (1MC) gust velocity profile, as shown in figure 6.

As prescribed by the "Certification Specification for Large Aeroplanes CS-25",[21] the shape of the gust has to be taken as:

$$W_g(x) = \begin{cases} \dfrac{U_{ds}}{2}\left(1 - cos\left(\dfrac{\pi x}{H}\right)\right) & for \;\; 0 \leq x \leq 2H \\ \\ 0 & otherwise \end{cases} \tag{54}$$

where x is the distance penetrated into the gust, U_{ds} is the design gust velocity in equivalent air speed (EAS), defined by Eq. (55), and H (in m) is the distance parallel to the flight path of the aeroplane for the gust to reach its peak velocity ($H = L_g/2$, half of the gust wavelength). The design gust velocity is then defined as:

$$U_{ds} = U_{ref} F_g \left(\frac{H}{106.68}\right)^{1/6} \tag{55}$$

where U_{ref} is the reference gust velocity in EAS and F_g is the flight profile alleviation factor. U_{ref} reduces linearly from 17.07 m/s EAS at sea level to 13.41 m/s EAS at 4572 m (15000 ft) and then again to 6.36 m/s EAS at 18288 m (60000 ft). In the following examples a value of F_g equal to 1 has been considered.

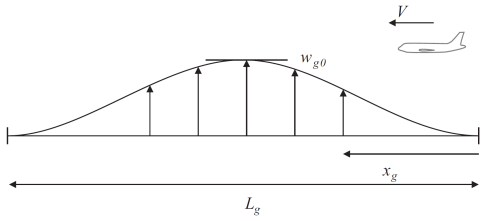

(a) $1 - \cos$ gust shape[22]

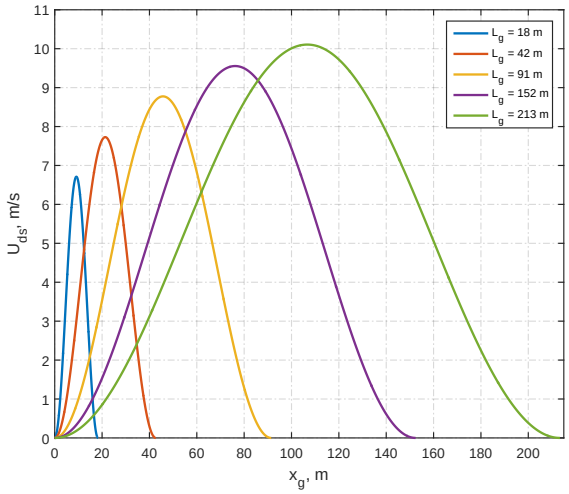

(b) Gust profile analysed.

Figure 6: Gust profile.

Two sets of gusts have been investigated to check the validity of the method for a cruise flight condition at $1g$ and altitude of 11000 m. The first is a low Mack number flight condition at $M = 0.5$. The second case consider a transonic flight condition at $M = 0.85$. See table 2 and figure 6b.

Table 2: "1-COS" gust profiles considered for gust loads response analysis, flight condition at $1g$ and altitude of 11000 m.

$AoA,\ deg$	$L_g,\ m$	$W_g^{EAS},\ m/s$	$W_g^{TAS},\ m/s$	M	$\alpha_g,\ deg$	$T_g,\ sec$	M	$\alpha_g,\ deg$	$T_g,\ sec$
0.0	18.28	6.71	12.29	0.50	4.76	0.124	0.85	2.81	0.073
0.0	42.67	7.73	14.15	0.50	5.48	0.289	0.85	3.23	0.170
0.0	91.44	8.77	16.07	0.50	6.22	0.620	0.85	3.67	0.365
0.0	152.40	9.55	17.50	0.50	6.77	1.033	0.85	3.99	0.608
0.0	213.36	10.11	18.51	0.50	7.15	1.446	0.85	4.22	0.851

The result comparing the total aerodynamic gust loads obtained for the five gust lengths are shown in figure 7. In these pictures only the delta loads have been reported, removing the steady aeroelastic load at trim. The results obtained by the correct DLM method have shown how it is possible to increase the accuracy of both the rigid gust and the flexible increment loads prediction. The corrected panel method is capable of matching the aerodynamic loads predicted by the fully coupled system for the short and medium gust length. For the long gust length the corrected DLM method tends to slightly overestimate the loads predicted by the FSI interface. This behaviour is due to the non linear effect that the correction approach can not predict in the present formulation. However, it is evident that the correction proposed can capture the right dynamic behaviour predicted by the FEM/CFD coupled solution.

Since the correction factors have shown a smooth variation with frequency, figure 9, it is possible to reduce the sampling points interpolating the correction factors. The CFD simulation can be performed for a selection of reduced frequency values, and then the correction factors can be extrapolated to the full series of k, table 1, by means of interpolation.

In figure 10, are presented the results obtained from the full corrected method and those obtained computing CFD simulations for only six frequencies and then using linear interpolation to obtain the remaining correction factors.

This interpolation approach wants just to highlight the possibility, but the final scope is to use an optimization approach to select the best sampling points to investigate with high fidelity methods.

IV. Conclusion

A correction method capable to increase the accuracy of the aerodynamic loads computed using the doublet-lattice method has been presented. The results for the static aeroelastic trim analysis and for the response to a "1-COS" gust shape have been presented. Five gusts length have been analysed among those prescribed by the regulation CS-25. The correction factors computed present a smooth behaviour with frequency and the results of an interpolation technique to reduce the sampling point has been shown. Investigation are on going to extend the presented method to a viscous case. Future works will try to include, in the corrected DLM, the effects of non linearity that at the moment are not captured.

Acknowledgments

The research leading to these results has received funding from the European Community's Marie Curie Initial Training Network (ITN) on Aircraft Loads Prediction using Enhanced Simulation (ALPES) FP7-PEOPLE-ITN-GA-2013-607911. The partners in the ALPES ITN are the University of Bristol, Siemens and Airbus Operations Ltd.

References

[1]E Albano and W. P. Rodden. A Doublet-Lattice Method for Calculating Lift Distributions on Oscillating Surfaces in Subsonic Flows. *AIAA Journal*, 7(2):279–285, 1969.

[2]W. P. Rodden and Paul F. Taylor. Improvements To the Doublet-Lattice Method in MSC Nastran. pages 1–16.

[3]W. P. Rodden, Paul F. Taylor, and Samuel C. McIntosh. Further Refinement of the Subsonic Doublet-Lattice Method, 1998.

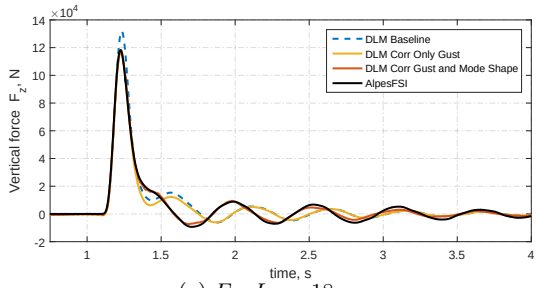

(a) F_z, $L_g = 18m$

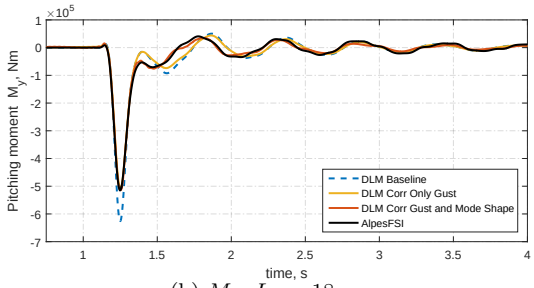

(b) M_y, $L_g = 18m$

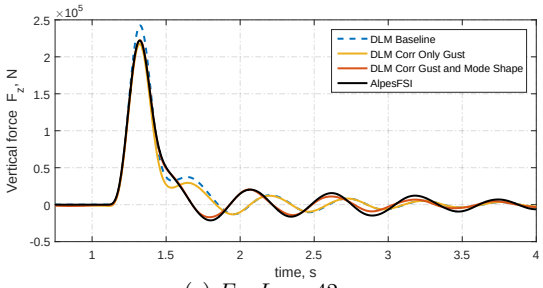

(c) F_z, $L_g = 42m$

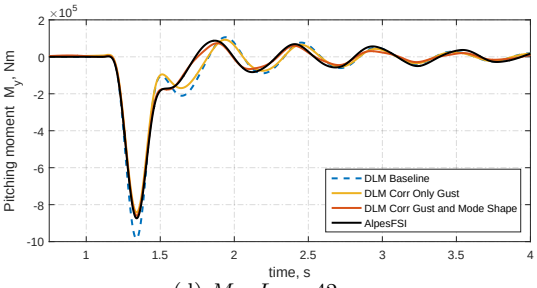

(d) M_y, $L_g = 42m$

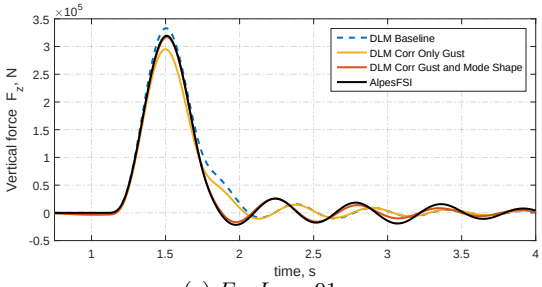

(e) F_z, $L_g = 91m$

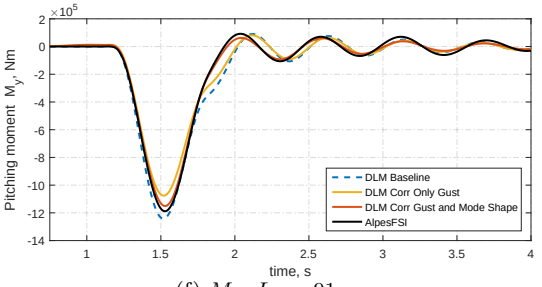

(f) M_y, $L_g = 91m$

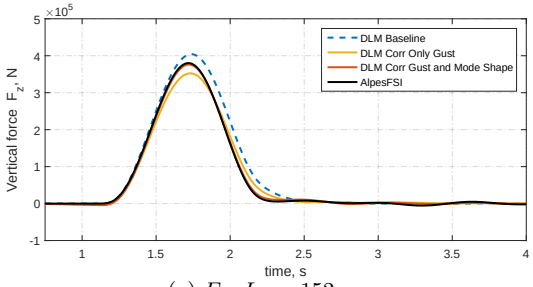

(g) F_z, $L_g = 152m$

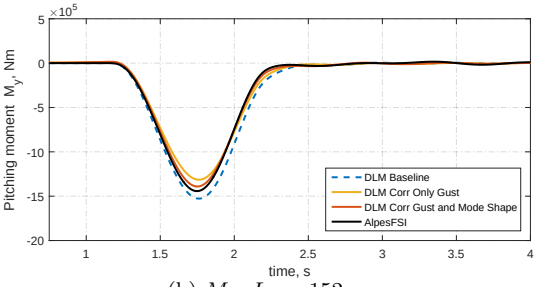

(h) M_y, $L_g = 152m$

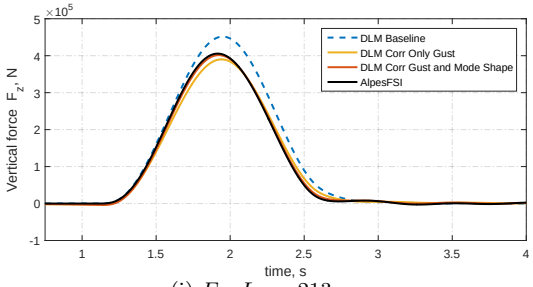

(i) F_z, $L_g = 213m$

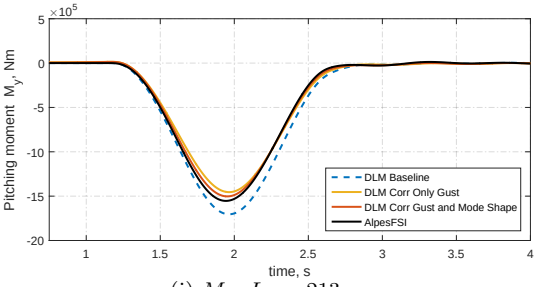

(j) M_y, $L_g = 213m$

Figure 7: Comparison of vertical force and pitching moment computed with Baseline DLM, Corrected DLM and Coupled CFD/FEM for low Mach number, $M = 0.50$.

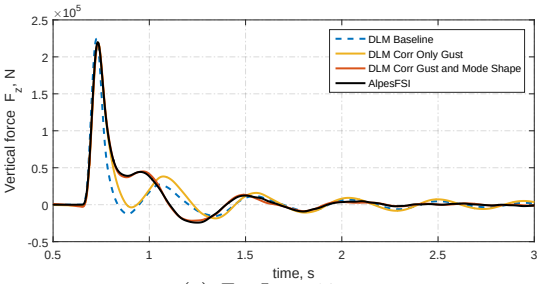

(a) F_z, $L_g = 18m$

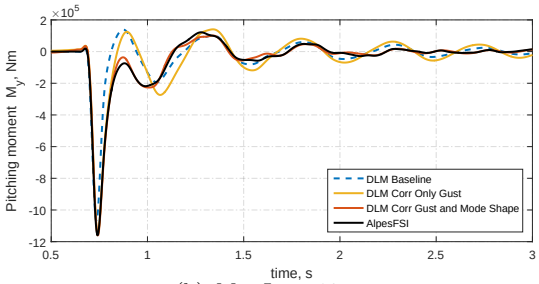

(b) M_y, $L_g = 18m$

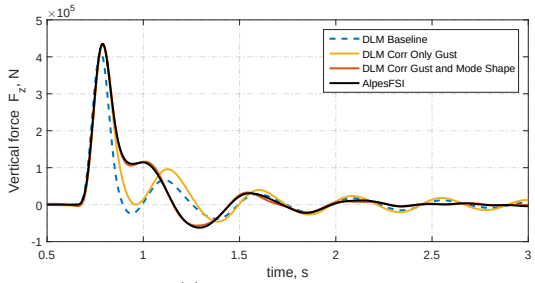

(c) F_z, $L_g = 42m$

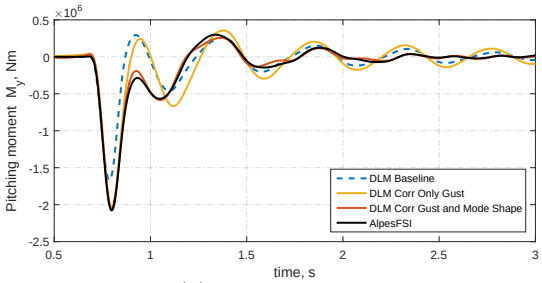

(d) M_y, $L_g = 42m$

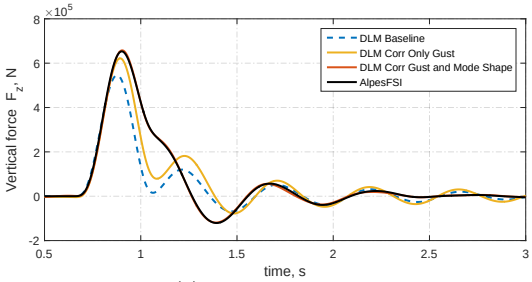

(e) F_z, $L_g = 91m$

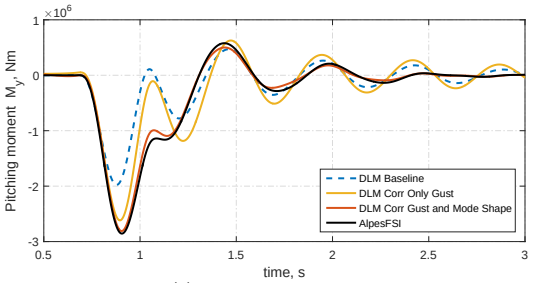

(f) M_y, $L_g = 91m$

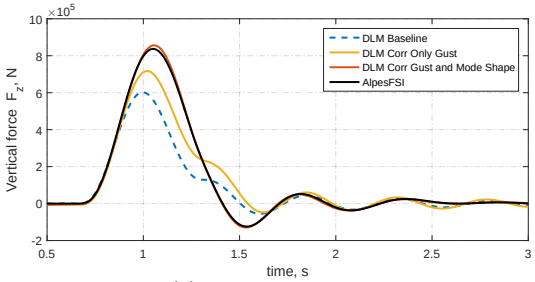

(g) F_z, $L_g = 152m$

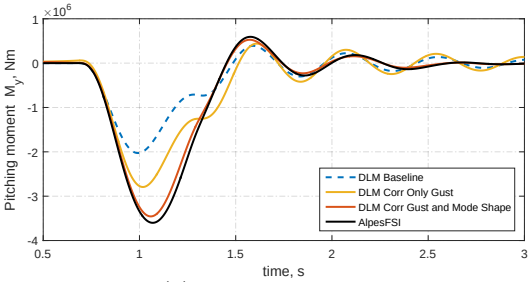

(h) M_y, $L_g = 152m$

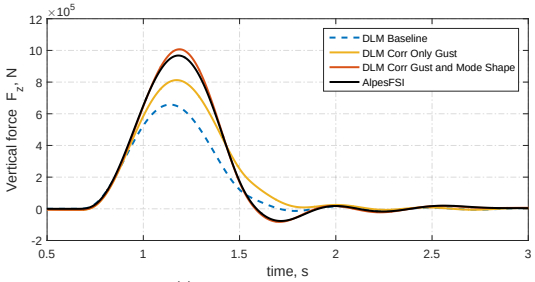

(i) F_z, $L_g = 213m$

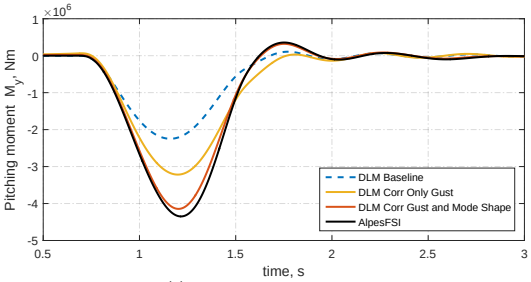

(j) M_y, $L_g = 213m$

Figure 8: Comparison of vertical force and pitching moment computed with Baseline DLM, Corrected DLM and Coupled CFD/FEM for high Mach number, $M = 0.85$.

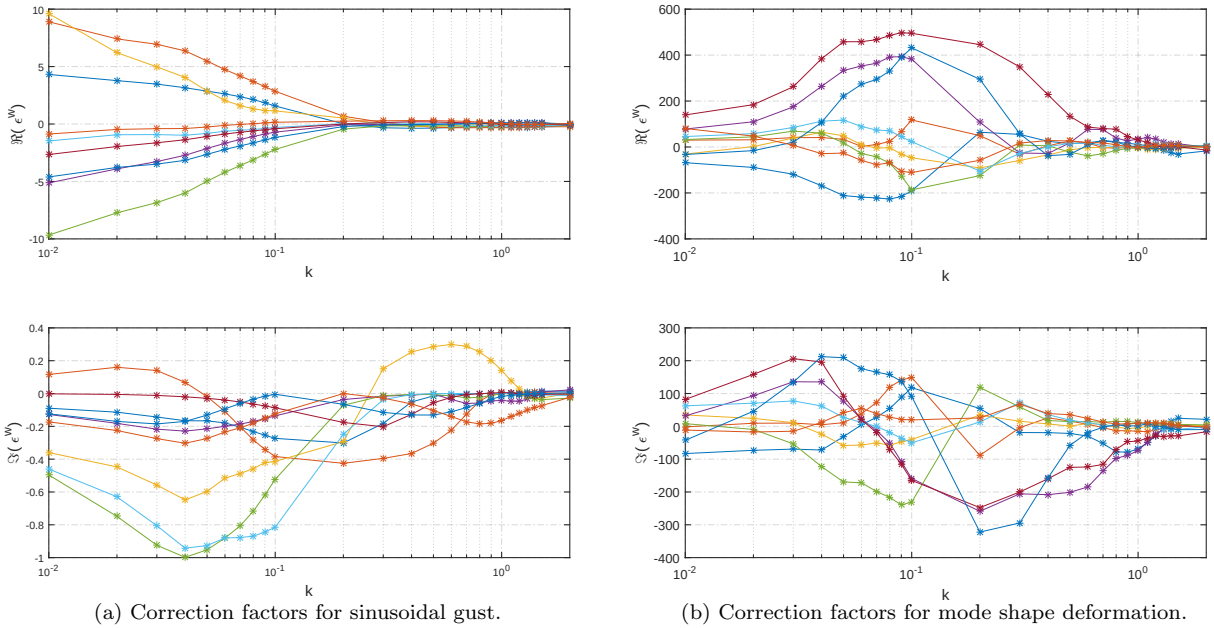

(a) Correction factors for sinusoidal gust. (b) Correction factors for mode shape deformation.

Figure 9: Real and imaginary part of the correction factors plot in function of the reduced frequency.

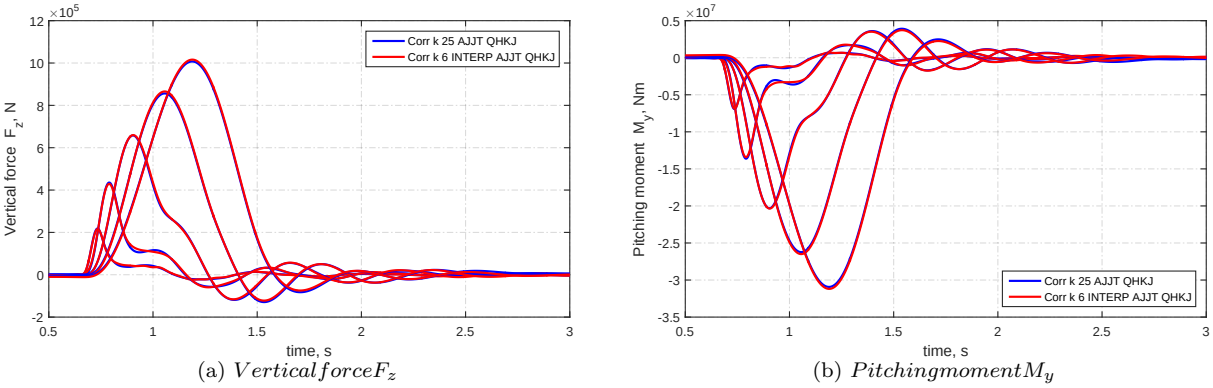

(a) $Vertical force F_z$ (b) $Pitching moment M_y$

Figure 10: Comparrison of vertical force and pitching moment for the five gusts length computed using the DLM corrected for all the reduced frequencies and for only 6 reduced frequencies.

[4]Rafael Palacios, H Climent, A Karlsson, and B Winzell. Assessment of strategies for correcting linear unsteady aerodynamics using CFD or experimental results. *International Forum on Aeroelasticity and Structural Dynamics (IFASD)*, 66(17 2), 2001.

[5]J. P. Giesing, T. P. Kalman, and W. P. Rodden. Correction Factor Techniques for Improving Aerodynamic Prediction Methods. 1976.

[6]Jan Brink-Spalink and J. M. Bruns. Correction of unsteady aerodynamic influence coefficients using experimental or CFD data. In *41st AIAA Conference Atlanta, GA*, 2000.

[7]Ralf Heinrich and N Kroll. Fluid-Structure Coupling for Aerodynamic Analysis and Design A DLR Perspective. *Most*, (January):1–31, 2008.

[8]Stefan Keye. Fluid-Structure-Coupled Analysis of a Transport Aircraft and Comparison to Flight Data. In *39th AIAA Fluid Dynaminamics Conference*, number 22-25 June 2009, pages 1–10, San Antonio, Texas, 2009.

[9]Bernd Stickan, Hans Bleecke, and Silvio Schulze. NASTRAN Based Static CFD-CSM Coupling in FlowSimulator. *Computational Flight Testing Notes on Numerical Fluid Mechanics and Multidisciplinary Design*, 123:223–234, 2013.

[10]Hendrik Tijdeman. *Investigations of the Transonic Flow Around Oscillating Airfoils*.

[11]Roberto Gil Annes Da Silva, Olympio A. F. Mello, João Luiz F. Azevedo, P. C. Chen, and D. D. Liu. Investigation on

Transonic Correction Methods for Unsteady Aerodynamics and Aeroelastic Analyses. *Journal of Aircraft*, 45(6):1890–1903, 2008.

[12]E. H. Johnson. MSC Nastran Version 68 Aeroelastic Analysis User's Guide - 2. *Structure*, 1994.

[13]Dorian Jones and Ann Gaitonde. Future Fast Methods for Loads Calculations : The FFAST Project. In *Innovation for Sustainable Aviation in a Global Environment proceedings of Aerodays*, pages pp. 110–115.

[14]Carmine Valente, Dorian Jones, Ann Gaitonde, J E Cooper, and Yves Lemmens. OpenFSI Interface For Strongly Coupled Steady And Unsteady Aeroelasticity. In *International Forum on Aeroelasticity and Strucutral Dynamics*, pages 1–16, Saint Petersburg, Russia, 2015.

[15]D. Schwamborn, T. Gerhold, and R. Heinrich. The DLR TAU-Code: Recent Applications in Research and Industry. *European Conference on Computational Fluid Dynamics, ECCOMAS CFD 2006*, pages 1–25, 2006.

[16]Ralf Heinrich. Comparison of different approaches for gust modeling in the cfd code tau. pages 1–12.

[17]Gowtham Jeyakumar and Dorian Jones. Aerofoil gust responses in viscous flows using prescribed gust velocities. Technical report, 2013.

[18]C. Wales, Dorian Jones, and A. Gaitonde. Prescribed Velocity Method for Simulation of Aerofoil Gust Responses. *Journal of Aircraft*, pages 1–13, 2014.

[19]P Bekemeyer and S Timme. Reduced Order Gust Response Simulation using Computational Fluid Dynamics. In *57th AIAA/ASCE/AHS/ASC Structures, Structural Dynamics, and Materials Conference*, number January, pages 1–13, San Diego, California, USA, 2016.

[20]Philipp Bekemeyer, Reik Thormann, and Sebastian Timme. Rapid Gust Response Simulation of Large Civil Aircraft using Computational Fluid Dynamics. In *Applied Aerodynamics Conference*, number July, pages 1–12, 2016.

[21]Easa. Certification Specifications for Large Aeroplanes CS-25. Technical Report 19 September, 2007.

[22]J. R. Wright and J. E. Cooper. *Introduction to Aircraft Aeroelasticity and Loads*. 2007.